International Journal for Housing Science and Its Applications
Publish August 10, 2025. Volume 46, Issue 4 Pages 4976-4986

https://doi.org/10.70517/ijhsa464341

# Concrete Mix Design Optimization Model Based on Particle Swarm Algorithm

**Nianlong Chi[1,*] and Liping Yan[1]**
[1] College of Civil Engineering, Fujian Chuanzheng Communications College, Fuzhou, Fujian, 350000, China
Corresponding authors: (e-mail: 18060484282@163.com).

**Abstract** Concrete as the basic material of construction project, its proportioning directly affects the project quality and cost. In this paper, a multi-objective optimization model for concrete proportioning is constructed, and an improved multi-objective particle swarm algorithm (IMOPSO) is proposed with the clinker three-rate value deviation and raw material cost as the optimization objectives. The algorithm improves the convergence and diversity of the solution through a dual external archiving mechanism and a two-stage global optimal selection strategy. On the ZDT standard test function, the IMOPSO algorithm achieves a convergence degree of 0.00355, which is significantly better than the NSGA-II and SPEA2 algorithms. The algorithm is applied to the optimization of 7 groups of ratios in a concrete enterprise, and the results show that compared with the NSGA-II algorithm, the running time of IMOPSO is shortened from an average of 90.29 seconds to 28.31 seconds, with an efficiency improvement of 68.6%; the cost of raw materials can be as low as 511.54 yuan/ton under the premise of ensuring that the quality control indexes meet the requirements. The study shows that the improved algorithm has higher solution accuracy and efficiency in solving the concrete ratio optimization problem, which provides an effective tool for intelligent decision-making in concrete production.

**Index Terms** Concrete proportioning, Multi-objective optimization, Particle swarm algorithm, Double external filing mechanism, Clinker triple rate value, Raw material cost

## I. Introduction

In the booming development of the construction industry, concrete products as the core foundation material, its quality is directly related to the safety and durability of the engineering structure [1]. Concrete constitutes the main body or skeleton of civil engineering and construction projects, which not only bears various loads, but also plays the functions of seepage prevention, heat insulation and heat preservation, and resists the erosion of the climate environment, so it must have sufficient durability [2]-[4]. However, with the rising quality requirements of concrete products in the construction market and the increasing pressure of cost control caused by the fluctuation of raw material prices, the traditional empirically determined concrete proportioning program has been difficult to meet the stringent demand for high-quality, low-cost concrete products in modern engineering construction [5]-[8]. In this context, the optimization of concrete proportioning research based on scientific analysis means is particularly critical and urgent to enhance the competitiveness of enterprise products and achieve sustainable development.

With the rapid development of computer technology, information technology and system technology, it is now possible to establish a complex nonlinear mathematical model of concrete properties based on existing test data, so as to predict the concrete strength [9]-[11]. However, due to the complexity of high-strength concrete grouping data, its prediction accuracy is poor [12]. And with the help of intelligent algorithms for the optimal design of high-performance concrete ratios, and then develop an intelligent decision-making system for the prediction of concrete performance and ratio optimization, so that the performance prediction modeling and ratio design computerization is an important development direction to improve the performance of concrete [13]-[16].

In this paper, a multi-objective optimization model with the objectives of minimizing the deviation of clinker three-rate value and minimizing the cost of raw materials is established from the actual demand of concrete production. In the algorithm design, an improved multi-objective particle swarm algorithm is formed by introducing a double external archive mechanism to enhance the preservation ability of the non-dominated solution, and adopting a two-stage selection strategy to improve the selection method of the global optimal solution. The performance of the algorithm is verified by the standard test function, and it is applied to the proportioning optimization of actual production data, with a view to providing technical support for the intelligent production of concrete enterprises.

## II. Multi-objective optimization study of concrete proportioning

### *II. A.Multi-objective optimization problem description and analysis*

Multi-objective optimization problems exist in many fields such as daily life and engineering practice, due to the mutual influence, mutual constraints and complex constraints between multiple objectives, resulting in the improvement of one sub-objective will reduce the effect of the other sub-objectives, so finding a solution to make each sub-objective achieve a satisfactory effect at the same time is the ultimate goal of multi-objective optimization problems [17].

In this paper, we focus on the case of minimizing the objective value of the sub-objectives, and the following is a mathematical description of this type of multi-objective optimization problem:

$$\min[f_1(x), f_2(x), f_3(x), \cdots, f_n(x)] \quad s.t. \begin{cases} x_{i\min} \le x_i \le x_{i\max} \\ Aeq * x = beq \\ A * x \le b \\ c(x) \le 0 \\ ceq(x) = 0 \end{cases} \tag{1}$$

where $x_i(i=1,2,\cdots,m)$ is the $m$-dimensional decision variable, $f_i(x)(i=1,2,\cdots,n)$ is the $n$-objective function to be optimized, $Aeq * x = beq$ is the linear equality constraint for the variable $x$, $A * x \le b$ is the variable $x$, $c(x) \le 0$ is a linear inequality constraint on the variable $x$, and $ceq(x) = 0$ is a nonlinear equality constraint on the variable $x$.

### *II. B.Multi-objective optimization model for concrete proportioning*

According to the multi-objective mathematical description, this section takes the actual production of A concrete enterprise as a starting point, and researches the establishment of a multi-objective optimization model for the raw fuel batching of raw concrete materials based on the process mechanism in view of the situation that the raw materials contain calorific value in the batching process. The final establishment of this optimization model is divided into three steps of optimization variable selection, objective function setting and constraints, and these three parts are introduced separately in the following.

#### II. B. 1) Optimization variable selection

When the optimization variable selection is carried out, the ratio of three main materials and two auxiliary materials is preferred because the main factor determining the clinker quality and production cost in the process of raw concrete batching is the ratio of raw materials. The raw material composition of the main materials selected in this chapter contains blast furnace slag, early-strength silicate cement, and fine sand, and the raw material composition of the auxiliary materials includes silica micropowder and naphthalene-based water reducing agent powder.

#### II. B. 2) Objective function establishment

The ultimate purpose of concrete raw material batching is to achieve qualified and stable clinker quality, and the key index to measure clinker quality is the clinker three-rate value: limestone saturation ratio coefficient (KH), silicon rate (SM) and aluminum rate (IM). The three-rate value represents the proportionality of each oxide content in clinker, as well as its internal mineral composition. Concrete companies prepare raw materials and calcine clinker by setting the clinker triple-rate value as a control target. Clinker can only be judged to be acceptable when all three values are within the fluctuation range of the target rate. The clinker three rate values are shown in the following formula.

(a) Limestone saturation ratio coefficient:

$$KH = \frac{C_c - 1.65 \times A_c - 0.35 \times F_c}{2 - 8 \times S_c} \tag{2}$$

(b) Silicon rate:

$$SM = \frac{S_c}{A_c + F_c} \tag{3}$$

(c) Aluminum rate:

$$IM = \frac{A_c}{F_c} \tag{4}$$

The $S_c, A_c, F_c, C_c$ in the formula represents the content of CaO, $SiO_2$, $Al_2O_3$ and $Fe_2O_3$ in clinker respectively. The three rate values are coupled with each other, in order to achieve a certain rate value to change the ratio of raw materials will certainly have an impact on other rate values. In this chapter, the deviation of clinker three rate values from the desired target value is used as the quality objective function to measure the multi-objective optimization of raw material batching. The three sub-objective functions are converted into one objective function by linear weighting, and the mathematical expressions are as follows:

$$\min f_1(X) = K_1(KH - KH^*)^2 + K_2(SM - SM^*)^2 + K_3(IM - IM^*)^2 \tag{5}$$

The $KH, SM, M$ in the formula is the calculated value of the three rate values, $KH^*, SM^*, M^*$ is the target rate value, and because the permissible range of deviation between the three rate values is inconsistent, $K_i (i = 1,2,3)$ is the value of the ratio coefficient setting.

Each raw material has different price and contained oxide content, increasing the proportion of a certain raw material will not only make the value of the three rates closer to the target value, but also cause changes in the cost of raw materials. In order to rationalize the deployment of mineral resources and reduce the cost price of raw materials, the cost function calculated in this paper is the cost per ton of compound, and the mathematical expression is as follows:

$$\min f_2(X) = \sum_{i=1}^{5} X_i Y_i \tag{6}$$

where $Y_i (i = 1,2,3,4,5)$ is the unit price of each raw material in yuan/ton.

**II. B. 3) Constraints**

(1) Raw Material Composition Baseline Constraints

Since coal-based materials are also involved in heat distribution, their chemical composition needs to be corrected so that their chemical composition can be converted to dry basis composition. The conversion formula is as follows:

$$cf_i = cf_i \times b_i \tag{7}$$

where $b_i (i = 1,2)$ is the percentage ash content in the material, and $cf_i (i = 1,2,\ldots,n)$ is the oxide composition of the material. The heat generation of coal material is $Q_i (i = 1,2)$ (unit: kJ/kgr).

(2) Mass conservation constraints

From the physical changes and chemical reactions in the clinker calcination process, it is known that if production losses are not considered, according to the principle of conservation of mass, the content of each oxide of the raw material under the dry base is equal to the sum of the composition of each dry base material. Although each major oxide exists in different forms, its total content remains unchanged. According to the conservation of mass the following relation is obtained:

$$\begin{bmatrix} S \\ A \\ F \\ C \end{bmatrix} = \begin{bmatrix} S_1 & S_2 & S_3 & b_1 S_4 & b_2 S_5 \\ A_1 & A_2 & A_3 & b_1 A_4 & b_2 A_5 \\ F_1 & F_2 & F_3 & b_1 F_4 & b_2 F_5 \\ C_1 & C_2 & C_3 & b_1 C_4 & b_2 C_5 \end{bmatrix} \begin{bmatrix} X_1 \\ X_2 \\ X_3 \\ X_4 \\ X_5 \end{bmatrix} \tag{8}$$

The $S_c, A_c, F_c, C_c$ in clinker can be obtained by converting the oxides in the above equation to a scorch base, so that $L_4, L_5$ is the loss on ignition of the coal research stone and the fuel coal, which is calculated by the following formula:

$$\begin{bmatrix} S_c \\ A_c \\ F_c \\ C_c \end{bmatrix} = \begin{bmatrix} S \\ A \\ F \\ C \end{bmatrix} \times (1 - \sum_{i=1}^{5} L_i X_i)^{-1} \tag{9}$$

The clinker triple rate value formula shows that $S_c, A_c, F_c, C_c$ are not involved in the calculation of the rate values when they are performed, $(1-\sum_{i=1}^{5} L_i X_i)^{-1}$ is not involved in the operation, and therefore $S, A, F, C$ can be directly substituted into the three-rate value formula.

(3) Energy conservation constraints

Since gangue is a raw material containing calorific value, it is used as both raw material and fuel in clinker production, so it needs to be considered to follow the principle of energy conservation in addition to satisfying the clinker composition in the process of batching calculation. According to the principle of conservation of energy, the total calorific value of coal material needs to meet the clinker firing heat consumption $Q$ (unit: kJ/kgr), the relationship is as follows:

$$X_4 Q_1 + X_5 Q_2 \le Q_{\max} \tag{10}$$

(4) Target range constraints

The clinker triple rate values that make up the quality target each have a qualifying range, and the saturation ratio $KH$ is allowed to fluctuate in the range of ±0.02, but its fluctuation range is ±0.01 in the batching calculation. Silicon rate $SM$ is allowed to fluctuate within ±0.1. Aluminum rate $IM$ is allowed to fluctuate within ±0.1. In the actual solution calculation, a qualified solution is required to bring all three rate values within the allowable range of the target rate value at the same time.

(5) Hazardous substance constraints

According to the requirements of harmful substance content of concrete clinker, MgO in clinker needs to be controlled within a certain range. Among them, the appropriate amount of MgO in clinker will increase the number of liquid phase and reduce its viscosity, which is conducive to the calcination C If too much, it will have a certain impact on the stability of concrete, so its content needs to be less than or equal to 7%. The calculation process of this substance is consistent with the calculation of the main oxides in clinker.

(6) Batching constraints

The batching calculation process contains only four raw materials and coal combustion, so its ratio sums up to 1, and the expression is as follows:

$$1 = \sum_{i=1}^{5} X_i \tag{11}$$

Based on the concrete production process and clinker composition, the upper and lower constraints on the proportion of each raw material are specified in actual production based on historical data, and the following are the ratio constraints for each material (i = 1, 2, 3, 4, 5):

$$X_{i\min} \le X_i \le X_{i\max} \tag{12}$$

## III. Multi-objective particle swarm algorithm and its improvement

### *III. A. Multi-objective particle swarm algorithm*

#### III. A. 1) Working Principle of Multi-Objective Particle Swarm Algorithm

Multi-objective particle swarm algorithm (MOPSO) is a simulation of the process of searching for food in a flock of birds, each particle is analogous to an individual bird, while the particle swarm is analogous to a flock of birds, the optimization objective function is equivalent to the food here, and all the particles are approaching to the objective function, forming an iterative process, the optimal solution corresponding to the particles in each iteration of updating is defined as an individual extremum ( $pbest$ ), and in this process the The whole population will also correspond to a population optimal value, defined as the global extreme value ( $gbest$ ), this optimization search process can be described by mathematical relations [18].

According to the principle of particle iteration in the multiobjective particle swarm algorithm, the velocity and position of the updated $k$ th generation particle $i$ are obtained as follows:

$$v_{id}^{k+1} = w \times v_{id}^{k} + c_1 \times r_1 (p_{id} - v_{id}^{k}) + c_2 \times r_1 (p_{gd} - v_{id}^{k}) \tag{13}$$

$$X_{id}^{k+1} = X_{id}^{k} + t \times v_{id}^{k+1} \tag{14}$$

where $v_{id}^{k}$ denotes the component of the velocity of particle $i$ in $d$ dimensions at $k$ iterations, $d = 1, 2, ..., n$, $n$ denotes the number of dimensions of the particle, $x_{id}^{k}$ denotes the $d$ -dimensional component of the particle $i$ 's

position at $k$ iterations, $P_{id}$ denotes the $d$-dimensional component of the particle $i$ itself at its best position, and $P_{gd}$ denotes the $d$-dimensional component of the population's best position.

The basic flow of the specific multi-objective particle swarm algorithm to solve the problem is shown in Figure 1.

Step1: Data initialization. Generate N populations in the space and set each parameter of the system.

Step2: Update the particle velocity and position, and determine the non-dominated solution set according to the domination relationship. Store the non-dominated solutions in the non-dominated solution set.

Step3: Calculate the value of the objective function and update the non-dominated solution set.

Step4: Determine the individual optimum as well as the global optimum based on the position velocity of the particle.

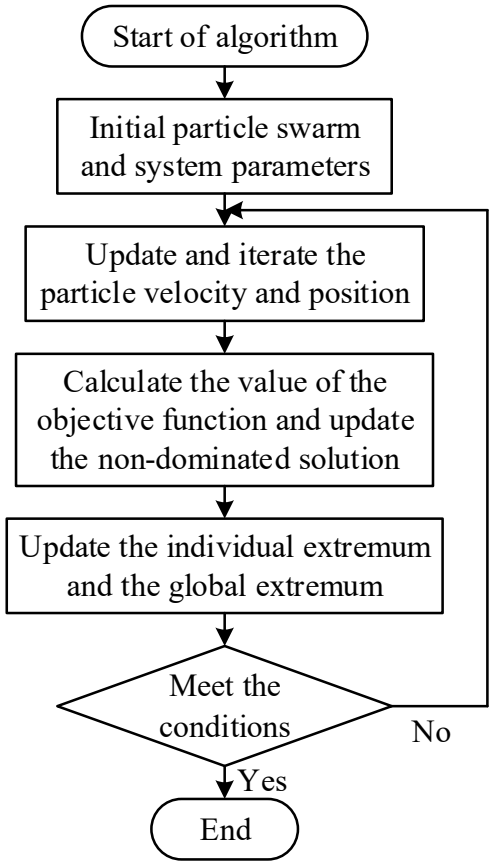


Figure 1: Basic flow chart of algorithm solution

**III. A. 2) External archiving mechanism**

The external archive is a collection used to store the optimal solution, from the beginning of the particle optimization until the process of finding the optimal solution requires a number of iterations to update, and the external archive is used to store the optimal solution of the update iteration in the optimization process. Specific algorithms use the external archive mechanism to realize the optimization steps are as follows:

(1) Initialize the algorithm, empty the external set and start the optimization search. First, the more dominant particles in the set of non-dominated solutions exist in the external set, followed by iterative optimization.

(2) At this time, the external set is a non-empty set, arbitrarily select one of the non-dominated solutions.

(3) Repeat the operation in (2) until the end of the algorithm iteration.

**III. A. 3) Selection of the global optimal solution**

The multi-objective particle swarm algorithm obtains multiple non-dominated Pareto optima, how to find the global optimum among multiple non-dominated solutions is an important part of the multi-objective particle swarm algorithm. In this algorithm, an external archive is obtained by the external archive mechanism, and the selection of global optimum is to be sought from this external archive. The more widely used is the dynamic field selection, that is, to determine an objective as the optimal, search for the nearest particles around it, compare the relevant particles

found with the second objective value of the particle, and select the particle with the smallest distance as the optimal solution, i.e., as the global optimal solution.

### *III. B. Improved multi-objective particle swarm algorithm*

#### III. B. 1) Improvements in external archiving mechanisms

In this paper, two external sets are established for storing non-dominated solutions, one as the main external storage set and the other as the auxiliary external storage set, and the auxiliary storage set is used to store particles with small crowding distances in the external storage set, and the main working principle is shown in Fig. 2. Set two external storage sets, as well as determine their capacity, when the main storage set reaches a certain capacity, then the particles deleted from the main storage set will be put into the auxiliary storage set, when the auxiliary storage set reaches the set capacity, the first particles added to it will be compared with the particles in the main storage set, and if this particle is the one with the smallest crowding distance, it will be deleted directly, and if this particle dominates the particles that are compared with it, then If this particle dominates the particles compared to it, it will be stored in the main storage set and the particles dominated by it will be deleted.

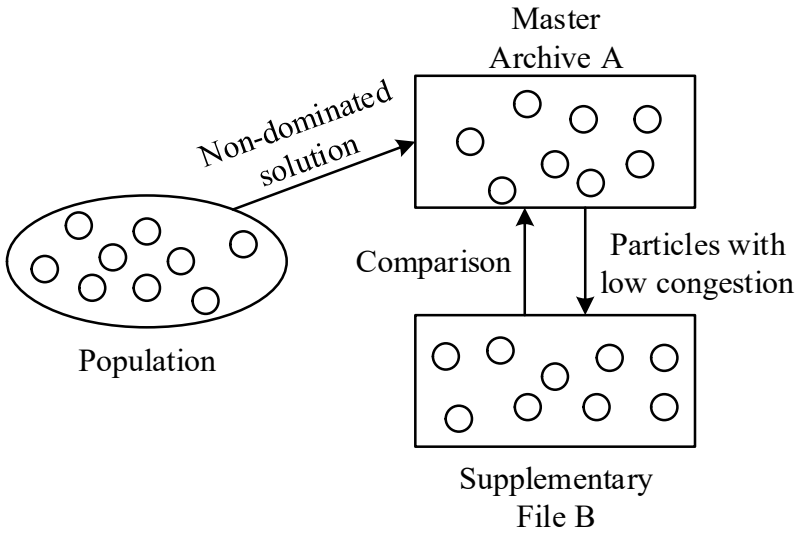


Figure 2: Schematic diagram of the dual archive mechanism

#### III. B. 2) Improvement of global optimal solution selection

As can be seen from 3.1.3, the selection of the global optimum in the unimproved multi-objective particle swarm algorithm is determined according to the dynamic domain selection mechanism, so that the global particles are difficult to jump out of the local optimum according to this selection method, and now the global optimum particles are selected by the two-stage shuffling selection strategy. The first stage is considered from the decision space and the second stage is considered from the goal space.

In the first stage of selection, the particles in the external file are analyzed and the following calculations are performed using the formula:

$$d(x_i, y_i) = \sqrt{\sum_{k=1}^{N} (x_{i,k} - y_{i,k})^2} \tag{15}$$

$$SD = \{d(x_i, y_1), d(x_i, y_2), ..., d(x_i, y_u)\} \tag{16}$$

where $x_i$ is the $i$ th particle, $y_j$ is the $j$ th non-dominated solution, $N$ is the particle dimension, and $u$ is the total number of non-dominated solutions. The computed result reflects the actual distance between the particles in the external file and the real particles in the Pareto face, and then the average similarity distance between that selected particle and the external document is computed according to Eq. (17), denoted as ASD, and the selected globally optimal particle must be smaller than the value of ASD:

$$ASD = \frac{\sum_{j=1}^{u} SD_{i,j}}{u} \tag{17}$$

The second stage is chosen to utilize the congestion distance for selection by first selecting the minimum value points of the multi-targets in the Pareto front surface to connect them, forming a plane with the points on other boundaries, calculating the distances from each point in the constituent plane to the extreme point, and taking the point with the largest distance as the global optimum to guide the overall particle flight.

## IV. Performance testing and simulation experiments

### *IV. A. Performance test of improved multi-objective particle swarm optimization algorithm*

In order to verify the arithmetic ability of the two methods on these functions before and after the improvement, three standard multi-objective test functions, ZDT1, ZDT2, and ZDT3, are used for comparison tests. The test functions are shown in Table 1.

Table 1: Test Functions

| Test function | Variable constraint | Target function | Functional dimension |
|---|---|---|---|
| ZDT1 | $0 \le x_i \le 1$<br>$i = 1, 2, \cdots, m$ | $F = (f_1, f_2)$<br>$f_1 = x_1$<br>$f_2 = g(1 - \sqrt{f_1 / g})$<br>$g = 1 + 9\sum_{i=2}^{m} x_i / (m-1)$ | m=30 |
| ZDT2 | $0 \le x_i \le 1$<br>$i = 1, 2, \cdots, m$ | $F = (f_1, f_2)$<br>$f_1 = x_1$<br>$f_2 = g(1 - (\sqrt{f_1 / g})^2)$<br>$g = 1 + 9\sum_{i=2}^{m} x_i / (m-1)$ | m=30 |
| ZDT3 | $0 \le x_i \le 1$<br>$i = 1, 2, \cdots, m$ | $F = (f_1, f_2)$<br>$f_1 = x_1$<br>$f_2 = g(1 - \sqrt{f_1 / g} - f_1 / g \sin x(10\pi f_1))$<br>$g = 1 + 9\sum_{i=2}^{m} x_i / (m-1)$ | m=30 |

The test results are shown in Figs. 3-5. The improved algorithm can converge well to the Pareto optimal front end of the test function.

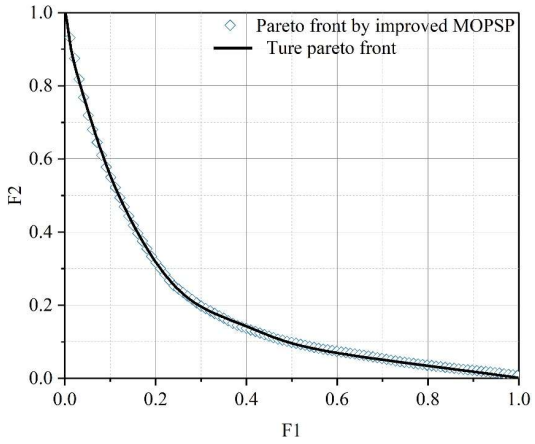


Figure 3: Simulation of ZDT1 with improved algorithm

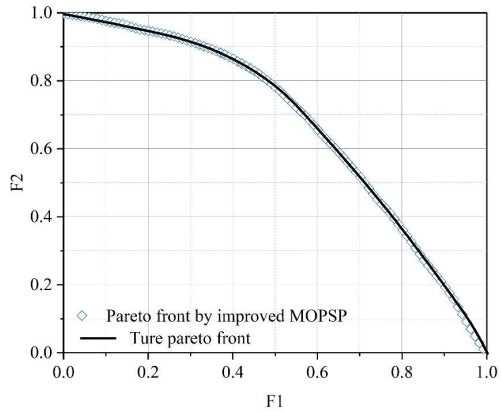


Figure 4: Simulation of ZDT2 with improved algorithm

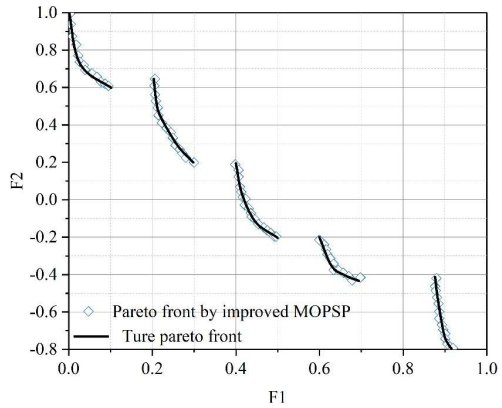


Figure 5: Simulation of ZDT3 with improved algorithm

In order to verify whether the improved algorithm has good convergence performance, it is compared with NSGA-II and SPEA2 respectively, and the results are shown in Table 2. From the test results, it can be observed that compared with the other two algorithms, the convergence degree of the improved MOPSO algorithm is the smallest on ZDT1, ZDT2 and ZDT3. The smaller convergence degree indicates that the Pareto solution solved by the algorithm is closer to the real frontier surface, and the distribution performance of the algorithm is more excellent, and the time required for computation is also the shortest among the three methods. The experimental results prove that the improved algorithm proposed in this paper has better convergence and diversity.

Table 2: Function comparison result

| Project | | ZDT1 | ZDT2 | ZDT3 |
|---|---|---|---|---|
| NSGA-II | Degree of convergence | 0.03103 | 0.02501 | 0.12964 |
| | Computation time/s | 3.163 | 3.085 | 2.417 |
| SPEA2 | Degree of convergence | 0.02129 | 0.01681 | 0.01784 |
| | Computation time/s | 2.427 | 2.873 | 2.578 |
| Improve MOPSO | Degree of convergence | 0.00609 | 0.00575 | 0.00355 |
| | Computation time/s | 1.999 | 2.166 | 2.087 |

### *IV. B. Experimental analysis*

After selecting the historical data of Concrete Plant A and calculating the equivalent values of raw material components using the system identification method, the improved MOPSO algorithm is used to solve the above raw material proportioning model, and the classical NSGA-II algorithm is selected as the comparison algorithm.

In order to ensure the fairness of the comparison results, the two algorithms are set to the same initialization state, the population size is 100, and the maximum number of iterations is 200.In this paper, a total of 7 sets of randomly calculated ratios, of which the Pareto optimal solution set obtained from a certain ratio using the improved MOPSO algorithm is shown in Figure 6.

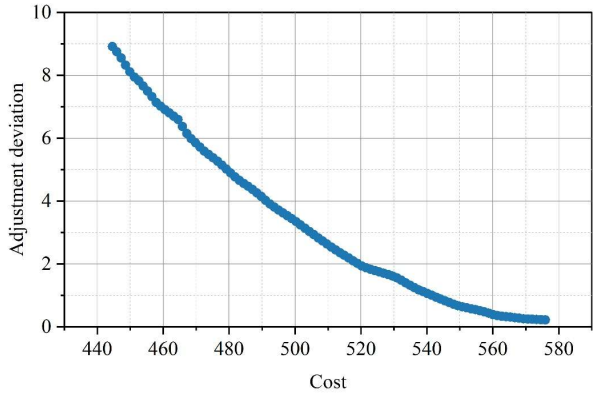


Figure 6: Pareto optimal solution set of a ratio

The range of five quality control objectives based on the optimal solution set is shown in Table 3.

Table 3: Quality control target range

| Control index | KH | SM | IM | Main material | Auxiliary material |
|---|---|---|---|---|---|
| Target range | 0.99±0.04 | 4.3±0.12 | 1.3±0.3 | 1.8±0.5 | 41±0.6 |

**IV. B. 1) Comparison of performance indicators**

In order to compare the performance of the algorithms more accurately, this paper selects the convergence and diversity of solutions to compare and analyze the algorithms.

(1) IGD evaluation index

IGD is the inverse generation distance, which reflects the distance between the non-dominated solution obtained by the algorithm and the front surface of the real solution, reflecting the convergence of the population, and the smaller the IGD is, the better the algorithm's convergence is.The specific expression for calculating IGD is shown in Eq. (18):

$$IGD(P^*, P) = \frac{\sum_{v \in p^*} d(v, p)}{|P^*|} \tag{18}$$

where $P*$ is a set of solutions falling on the Pareto front, $P$ is a set of non-dominated solutions, $v$ is a particle in $P*$, and $d(v, p)$ is the minimum distance from $v$ to $p$.

(2) SP evaluation metric

SP is a measure of the diversity of the obtained nondominated solutions, the measure of the variance of the minimum distance from each solution to the other solutions, the smaller the SP, the better the diversity of the solutions.The formula of SP is as in equation (19):

$$SP = \sqrt{\frac{1}{n-1} \sum_{i=1}^{n} (d_{mean} - d_i)} \tag{19}$$

where $d_{mean}$ is the average of $d_i$. $d_i = \min_j (\sum_{k=1}^{m} \left| f_k^i - f_k^i \right|), i, j = 1, \cdots, n, n$ is the number of non-dominated solutions.

Apply IMOPSO and NSGA-II to randomly solve 7 times raw material rationing to get Pareto optimal solution set. The results of the mean and standard deviation of the IGD metrics after applying the two algorithms to solve each of the seven ingredient ratios for 30 times are shown in Table 4.The IGD of IMOPSO is smaller, which indicates better convergence of the algorithms.

The SP values of the two algorithms are shown in Table 5. the SP of IMOPSO is smaller, indicating better diversity of solutions for the IMOPSO algorithm.

Table 4: IGD comparison between IMOPSO and NSGA-II

| Model | Control index | Proportioning | | | | | | |
|---|---|---|---|---|---|---|---|---|
| | | 1 | 2 | 3 | 4 | 5 | 6 | 7 |
| IMOPSO | Mean | 1.07 | 0.91 | -0.01 | 0.21 | 0.08 | 0.01 | 0.13 |
| | Std | 2.77 | 22.58 | 1.98 | 2.33 | 0.58 | 1.11 | 0.49 |
| NSGA-II | Mean | 1.08 | 1.48 | 0.54 | 0.24 | 0.58 | 0.41 | 0.61 |
| | Std | 5.08 | 23.17 | 11.09 | 3.33 | 7.96 | 6.07 | 8.56 |

Table 5: SP comparison between IMOPSO and NSGA- II

| Model | Proportioning | | | | | | |
|---|---|---|---|---|---|---|---|
| | 1 | 2 | 3 | 4 | 5 | 6 | 7 |
| IMOPSO | 1.14 | 0.37 | 0.3 | 0.35 | 0.19 | 0.24 | 0.29 |
| NSGA-II | 1.39 | 1.69 | 0.83 | 0.49 | 0.27 | 0.57 | 0.18 |

**IV. B. 2) Comparison of running times**

The average running time of the two algorithms for seven matching solvers is shown in Table 6. IMOPSO has a shorter solving time and is more efficient in solving.

Table 6: Comparison of running time between IMOPSO and NSGA- II

| Model | Proportioning | | | | | | |
|---|---|---|---|---|---|---|---|
| | 1 | 2 | 3 | 4 | 5 | 6 | 7 |
| IMOPSO | 7.32 | 33.23 | 72.74 | 1.63 | 22.32 | 24.3 | 36.65 |
| NSGA-II | 69.99 | 79.26 | 91.28 | 101.47 | 96.88 | 99.1 | 94.07 |

**IV. B. 3) Comparison of final proportioning results**

The seven sets of final ratios obtained by the two algorithms were used to calculate the predicted values of the five quality control objectives, and then the values of each comparison parameter were obtained and compared with the actual manual ratios. The comparison data are shown in Table 7.

Table 7: Comparison of Final Mix Ratio of IMOPSO, NSGA-II and Artificial match

| Method | Control index | Proportioning | | | | | | |
|---|---|---|---|---|---|---|---|---|
| | | 1 | 2 | 3 | 4 | 5 | 6 | 7 |
| IMOPSO | KH | 1.1 | 0.804 | 1.01 | 0.944 | 0.972 | 1.137 | 0.986 |
| | SM | 3.98 | 4.16 | 4.28 | 4.09 | 4.18 | 4.12 | 3.99 |
| | IM | 1.18 | 1.22 | 1.23 | 1.28 | 1.19 | 1.21 | 0.99 |
| | Main material | 44.15 | 44.28 | 43.79 | 43.6 | 43.67 | 43.75 | 44.34 |
| | Auxiliary material | 1.66 | 1.72 | 1.78 | 1.67 | 1.69 | 1.61 | 1.7 |
| | Cost | 617.14 | 610.93 | 530.28 | 567.34 | 531.91 | 599.35 | 511.54 |
| NSGA-II | KH | 0.827 | 0.917 | 1.107 | 0.905 | 0.972 | 1.046 | 1.103 |
| | SM | 3.97 | 4.02 | 4.19 | 3.96 | 3.98 | 4.02 | 4.08 |
| | IM | 1.21 | 1.29 | 1.18 | 1.28 | 1.36 | 1.13 | 1.3 |
| | Main material | 43.35 | 44.28 | 43.54 | 43.74 | 43.48 | 43.74 | 44.27 |
| | Auxiliary material | 1.63 | 1.42 | 1.8 | 1.59 | 1.44 | 1.73 | 1.57 |
| | Cost | 612.58 | 629.56 | 593.94 | 580.57 | 565.89 | 592.53 | 557.71 |
| Artificial matching | KH | 0.956 | 0.972 | 0.802 | 0.74 | 0.908 | 0.96 | 0.758 |
| | SM | 4.14 | 3.38 | 3.72 | 3.89 | 3.45 | 4.07 | 3.75 |
| | IM | 1.13 | 1.42 | 1.14 | 1.21 | 1.18 | 1.23 | 1.08 |
| | Main material | 43.81 | 43.17 | 43.51 | 44.1 | 44.09 | 44.82 | 43.76 |
| | Auxiliary material | 1.7 | 1.82 | 1.68 | 1.57 | 1.6 | 1.74 | 1.73 |
| | Cost | 616.57 | 586.8 | 611.41 | 569.58 | 599.08 | 596.04 | 535.4 |

From the experimental results, it can be seen that the Pareto solution obtained by IMOPSO algorithm outperforms NSGA-II in terms of both performance measures and algorithm runtime for ratio solving, and for the final ratios, the two algorithms are able to control all the control parameters within the target range compared to manual ratios. For the cost of raw materials, the final ratio obtained by IMOPSO algorithm can better reduce the cost of raw materials compared with NSGA-II solving ratio and manual ratio. Therefore, the IMOPSO algorithm proposed in this paper can be effectively applied in the optimization of raw material ratio solving, which reduces the ratio cost and improves the qualification rate of raw materials.

## V. Conclusion

In this study, the intelligent optimization of proportioning scheme is realized by establishing a multi-objective optimization model of concrete proportioning and proposing an improved multi-objective particle swarm algorithm. In the standard test function validation, the convergence of the improved algorithm on ZDT1, ZDT2 and ZDT3 reaches 0.00609, 0.00575 and 0.00355, respectively, and the computation time is controlled to be less than 2.166 seconds, with the comprehensive performance significantly better than the comparison algorithm. In the practical application of a concrete enterprise, the improved algorithm is used to optimize seven groups of ratios, and the quality control indexes of the resulting scheme meet the target requirements: the limestone saturation ratio coefficient is maintained between 0.804 and 1.137, the silica rate is stabilized in the range of 3.98 and 4.28, and the aluminum rate is controlled between 0.99 and 1.28. In terms of economic benefits, the optimized raw material cost was significantly reduced, in which the cost of rationing scheme 3 was only 530.28 yuan/ton, saving 13.2% compared with the traditional method. The improved multi-objective particle swarm algorithm effectively balances the contradiction between quality and cost in concrete proportioning, and provides a reliable technical solution for the intelligent production of construction materials, which has good engineering application prospects.

## References


[1] Benghida D. (2017). Concrete as a sustainable construction material. Key Engineering Materials, 744, 196-200.

[2] Zhou, M., Lu, W., Song, J., & Lee, G. C. (2018). Application of ultra-high performance concrete in bridge engineering. Construction and Building Materials, 186, 1256-1267.

[3] Klyuev, S. V., Klyuev, A. V., & Vatin, N. I. (2018). Fiber concrete for the construction industry. Magazine of Civil Engineering, (8 (84)), 41-47.

[4] Lee, D., Lee, D., Lee, M., Kim, M., & Kim, T. (2020). Analytic hierarchy process-based construction material selection for performance improvement of building construction: The case of a concrete system form. Materials, 13(7), 1738.

[5] DeRousseau, M. A., Kasprzyk, J. R., & Srubar Iii, W. V. (2018). Computational design optimization of concrete mixtures: A review. Cement and concrete research, 109, 42-53.

[6] Jafari, K., Tabatabaeian, M., Joshaghani, A., & Ozbakkaloglu, T. (2018). Optimizing the mixture design of polymer concrete: An experimental investigation. Construction and Building Materials, 167, 185-196.

[7] Ziaei-Nia, A., Shariati, M., & Salehabadi, E. (2018). Dynamic mix design optimization of high-performance concrete. Steel and Composite Structures, An International Journal, 29(1), 67-75.

[8] Rashid, K., Rehman, M. U., de Brito, J., & Ghafoor, H. (2020). Multi-criteria optimization of recycled aggregate concrete mixes. Journal of Cleaner Production, 276, 124316.

[9] Menna, C., Mata-Falcón, J., Bos, F. P., Vantyghem, G., Ferrara, L., Asprone, D., ... & Kaufmann, W. (2020). Opportunities and challenges for structural engineering of digitally fabricated concrete. Cement and Concrete Research, 133, 106079.

[10] Yaseen, Z. M., Tran, M. T., Kim, S., Bakhshpoori, T., & Deo, R. C. (2018). Shear strength prediction of steel fiber reinforced concrete beam using hybrid intelligence models: a new approach. Engineering Structures, 177, 244-255.

[11] Zhu, Y., Huang, L., Zhang, Z., & Bayrami, B. (2022). Estimation of splitting tensile strength of modified recycled aggregate concrete using hybrid algorithms. Steel and Composite Structures, An International Journal, 44(3), 389-406.

[12] Chen, B., Wang, L., Feng, Z., Liu, Y., Wu, X., Qin, Y., & Xia, L. (2023). Optimization of high-performance concrete mix ratio design using machine learning. Engineering Applications of Artificial Intelligence, 122, 106047.

[13] Zheng, W., Shui, Z., Xu, Z., Gao, X., & Zhang, S. (2023). Multi-objective optimization of concrete mix design based on machine learning. Journal of Building Engineering, 76, 107396.

[14] Sharifi, E., Sadjadi, S. J., Aliha, M. R. M., & Moniri, A. (2020). Optimization of high-strength self-consolidating concrete mix design using an improved Taguchi optimization method. Construction and Building Materials, 236, 117547.

[15] Zhang, J., Huang, Y., Wang, Y., & Ma, G. (2020). Multi-objective optimization of concrete mixture proportions using machine learning and metaheuristic algorithms. Construction and Building Materials, 253, 119208.

[16] Kurda, R., de Brito, J., & Silvestre, J. D. (2019). CONCRETop-A multi-criteria decision method for concrete optimization. Environmental Impact Assessment Review, 74, 73-85.

[17] Upadhayay Ashutosh,Ghosh Debdas,Ansari Qamrul Hasan & Jauny. (2022). Augmented Lagrangian cone method for multiobjective optimization problems with an application to an optimal control problem. Optimization and Engineering,24(3),1633-1665.

[18] Zhe Zhang,Shi Cheng,Yuyuan Shan,Zhixin Wang,Hao Ran & Lining Xing. (2024). Solving Multi-Objective Satellite Data Transmission Scheduling Problems via a Minimum Angle Particle Swarm Optimization. Symmetry,17(1),14-14.